

Passive Vibration Suppression in Truss-Type Structures with Tubular Members

Ramesh B. Malla,* Hamid R. Adib-Jahromi,† and Michael L. Accorsi‡
University of Connecticut, Storrs, Connecticut 06269

A method for vibration suppression using viscous damping material has been developed for truss structures consisting of axisymmetric tubular members of circular cross section. The vibration damping scheme calls for the construction of a structural member with two or more tubes by overlapping the end portion of adjacent tubes and bonding them together by means of a thin layer of viscoelastic material. The equations of motion for a finite length section consisting of concentric layers of an inner tube, viscous material damping layer, and outer tube are obtained using Hamilton's principle. Only axial motion is considered. An exact solution to the equation is obtained and used to develop the dynamic stiffness matrix for the section. A scheme has been presented to develop a super element that consists of two or more such damping sections. The super elements have then been used to model members in a truss-type structure to study the vibration suppression in the structure. The vibration suppression is studied for a range of frequencies. A parametric study has been performed to establish the effects of thickness, loss factor, and length of overlap. The study has shown that the damping effectiveness is dependent on the coupled effects of these parameters.

Nomenclature

A_i^*	= constants ($i = 1, 4$)
D	= dynamic stiffness matrix
Dom	= frequency sweep size (Fig. 12), Hz
E	= modulus of elasticity of the structural material
E_c	= complex modulus of elasticity of the viscous material
E_c^o	= storage modulus of elasticity of the viscous material
F_i	= end forces ($i = 1, 4$) (Fig. 3)
f_i	= parameter function of material and geometric properties and structural frequency ($i = 1, 2$)
G_c	= shear modulus of the viscoelastic material
G_c^o	= storage shear modulus of the viscoelastic material
h	= thickness
L	= length of a segment
l_c	= length of damping treatment
N_i	= magnitude of axial forces ($i = 1, 4$)
$n(z, t)$	= axial force (Fig. 3)
r	= radius
T	= kinetic energy
U	= strain energy
u, v, w	= displacements in the radial r , circumferential θ , and axial z directions, respectively
W_i	= magnitude of longitudinal (z direction) displacements ($i = 1, 4$)
δ	= vector of end displacements
δ_i	= end displacements ($i = 1, 4$) (Fig. 3)
ϵ	= vector of strain components
η	= loss factor of the viscous material
λ_i	= parameters (functions of material and geometric properties and structural frequency) ($i = 1, 2$)
ν	= Poisson's ratio
ρ	= density of the material
σ	= vector of stress components
ω	= structural natural frequency

Subscripts

1, 2, c = outer tube, inner tube, and viscous layer, respectively

Superscripts

$/$ = derivative with respect to z

\cdot = time derivative of the corresponding parameter

Introduction

LARGE space structures are inherently flexible and are susceptible to vibration. Vibration control can be achieved by active and/or passive techniques. In active control, sensors and actuators are mounted externally on the structure. Design requires knowledge of elastic modal frequencies and modal shapes at the location of the sensors and actuators. The interaction between the structure and the active control system is of considerable importance.

In passive damping, the inherent damping of the structure is augmented by incorporating high-damping material in the structure. Significant damping benefits can be achieved by incorporating viscoelastic materials in structural supports and connections.^{1,2} Numerous investigations on vibration, stress analysis, and dynamic modeling have been reported on sandwich construction of beams and plates and on single- and double-lap and scarf joints.^{3–17} For example, He and Rao¹⁴ developed a model to study damping under longitudinal vibration of an adhesively bonded double-lap joint and studied the effects of damping on the joint system behavior. The model studied by He and Rao is limited to only an individual joint and is useful for beams. Prucz et al.^{11,12} designed and tested new types of passively damped joints.

For truss structures, augmented damping is possible in the joints and in members. The effect of joint damping has been studied by Crawley,¹⁸ Belvin,¹⁹ and Bowden and Dugundji.²⁰ Member damping has been studied by several authors using various analytical methods^{21–24} Sankar and Deshpande²⁴ also utilized the dynamic stiffness matrix to evaluate the natural frequencies, mode shapes, and modal loss factor of a truss with several viscously damped members. In the study, however, the mass and, hence, the kinetic energy of the viscous layer were neglected.

Because of their light weight, relatively high stiffness, and ease of construction, truss-type structures are the preferred candidates for various types of applications in space.²⁵ Truss structures are also widely used on the Earth, especially for large-span construction projects. Tubular members of circular cross section are preferred for such construction, especially for space applications.²⁶ Work on the static stress analysis of adhesively bonded tubular lap joints under

Received 27 February 1998; revision received 9 September 1998; accepted for publication 6 July 1999. Copyright © 1999 by the authors. Published by the American Institute of Aeronautics and Astronautics, Inc., with permission.

*Associate Professor, Department of Civil and Environmental Engineering, Senior Member AIAA.

†Graduate Assistant; currently Principal, The SLAM Collaborative, 80 Glastonbury Boulevard, Glastonbury, CT 06033.

‡Associate Professor, Department of Civil and Environmental Engineering.

longitudinal and torsional loadings has been reported.^{27–31} Some of these studies considered the adhesive as viscoelastic material. More recently, vibration and damping analyses of tubular lap joints bonded by viscoelastic material have been presented.^{32,33} However, they deal with either the joint under torsion or beam-type flexural vibration. These are not suitable for a truss member that is primarily under axial motion. In addition, these studies are limited to the element level and not applied to a full structural system.

Therefore, the aim of the present study is to develop a passive damping scheme specialized for a total truss-type structure having circular-cross-section members. The technique calls for construction of a structural member from two or more circular tubes by overlapping the end portions and connecting them with viscoelastic material. An exact dynamic stiffness matrix is derived for a finite length section of a structural member made of three concentric circular tubes containing a viscous damping layer between the inner and outer tubes. Several such elements are then assembled to obtain a super element representing a full-length member of a truss structure. The basic composite damping elements can be assembled with a variety of configurations to achieve desired damping effects. Only axial motion is considered (truss members, no bending). The super elements are then used as web (vertical and diagonal) members in a truss-type structure, and the dynamic response of the structure is evaluated. Parameters of the damping layer are varied to study the effects of the damping scheme. Results are compared with those of a conventional finite element model.

Equations of Motion

Figure 1 illustrates the truss element treated in this study, which consists of an assembly of concentric tubes: an inner tube, an outer

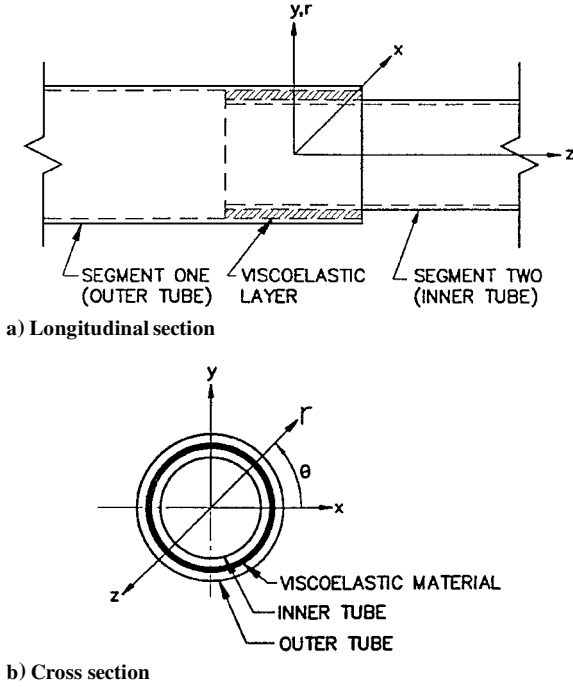


Fig. 1 Typical damping-treated truss member.

tube, and a viscoelastic layer between them. All tubular layers are assumed to be linear elastic and isotropic. Damping is included in the viscoelastic layer through the use of a loss factor and complex modulus of elasticity and shear modulus. To derive the equations of motion for the damping element (overlapped segment), expressions for the kinetic energy T and strain energy U in cylindrical coordinates (r, θ, z) are written to be incorporated into Hamilton's principle. The total kinetic and strain energies of the composite element is the sum of the kinetic energies for each layer. Figure 2 shows the free-body diagram of a structural member with three elements, one (the center one) being the overlapped portion containing the viscoelastic damping layer. Defining u, v , and w to be displacements in the radial, circumferential, and axial directions, respectively, it is assumed that $u = v = 0$ and $w = w(r, z)$ for each layer of the axisymmetric element. For the outer and inner tubes, the axial displacements along the radial direction are considered to be constant, whereas for the viscoelastic layer the axial displacement is assumed to vary linearly in the radial direction. Detailed derivations leading to the equations of motion can be found by Adib-Jahromi³⁴ and Adib-Jahromi et al.³⁵ For completeness of the material presented, the equations of motion for the three-layer damping element are presented hereafter.

Equations of motion for the overlap portion (damping element) of the tubular member are derived using Hamilton's principle. The following two equations of motion and associated natural boundary conditions are obtained:

$$2(A_1 r_1 h_1 + A_c a)w_1'' + A_c c w_2'' - 2\pi(\rho_1 r_1 h_1 + \rho_c a)\ddot{w}_1 - \pi\rho_c c \ddot{w}_2 - (2\pi G_c r_c / h_c)(w_1 - w_2) = 0 \quad (1)$$

$$2(A_2 r_2 h_2 + A_c b)w_2'' + A_c c w_1'' - 2\pi(\rho_2 r_2 h_2 + \rho_c b)\ddot{w}_2 - \pi\rho_c c \ddot{w}_1 - (2\pi G_c r_c / h_c)(w_2 - w_1) = 0 \quad (2)$$

The associated natural boundary conditions are

$$[2(A_1 r_1 h_1 + A_c a)w_1' + c A_c w_2' - n_1] \delta w_1|_{z=\pm L/2} = 0 \quad (3)$$

$$[2(A_2 r_2 h_2 + A_c b)w_2' + c A_c w_1' - n_2] \delta w_2|_{z=\pm L/2} = 0 \quad (4)$$

where the quantities a, b , and c are given as

$$a = (4r_c h_c + h_c^2)/12, \quad b = (4r_c h_c - h_c^2)/12 \quad (5)$$

$$c = (4r_c h_c)/12$$

and the quantity A_i ($i = 1, 2$, or c) is expressed as

$$A_i = \frac{\pi E_i (1 - \nu_i)}{(1 + \nu_i)(1 - 2\nu_i)} \quad (6)$$

Damping is included in the viscoelastic layer using a complex modulus of elasticity E_c and complex shear modulus G_c :

$$E_c = E_c^0 (1 + i\eta) \quad (7)$$

$$G_c = G_c^0 (1 + i\eta) \quad (8)$$

where η is the loss factor of the viscous material that indicates the fraction of strain energy lost in one cycle of the vibration.³⁶

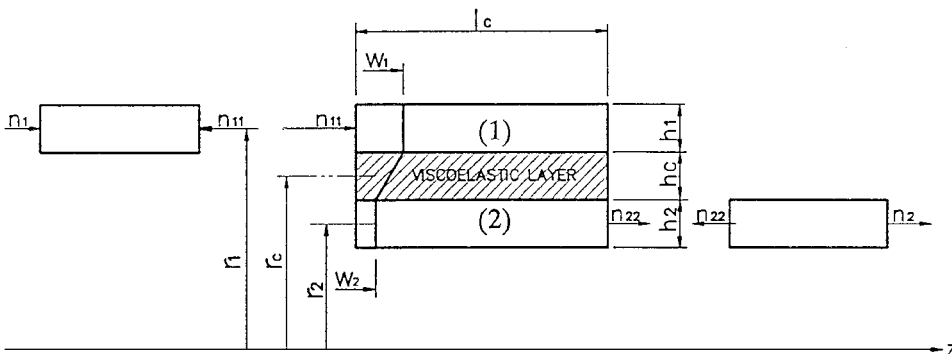


Fig. 2 Kinematic assumptions and free-body diagram.

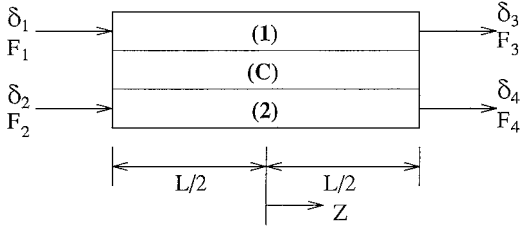


Fig. 3 End forces and displacements on a section.

Solution

The harmonic, time-dependent solution is obtained by assuming w_1, w_2, n_1 , and n_2 in the following form:

$$\begin{aligned} w_1(z, t) &= W_1(z)e^{i\omega t}, & w_2(z, t) &= W_2(z)e^{i\omega t} \\ n_1(z, t) &= N_1(z)e^{i\omega t}, & n_2(z, t) &= N_2(z)e^{i\omega t} \end{aligned} \quad (9)$$

Substituting these expressions into the equations of motion and assuming $W_1(z)$ and $W_2(z)$ of the form

$$W_1(z) = A_1^* \cosh(\lambda_1 z) + A_2^* \sinh(\lambda_1 z) + A_3^* \cosh(\lambda_2 z) + A_4^* \sinh(\lambda_2 z) \quad (10)$$

$$W_2(z) = A_1^* f_1 \cosh(\lambda_1 z) + A_2^* f_1 \sinh(\lambda_1 z) + A_3^* f_2 \cosh(\lambda_2 z) + A_4^* f_2 \sinh(\lambda_2 z) \quad (11)$$

λ_i ($i = 1, 2$) and f_i ($i = 1, 2$) can be computed. Both λ_i and f_i are functions of material and geometric properties and the structural frequency ω . The constants A_i^* ($i = 1, 4$) can be evaluated using the prescribed displacement or force boundary conditions. It will be more useful to eliminate the constants A_i^* and relate the unknown end displacements δ_i , $i = 1, 4$ (Fig. 3) and forces F_i , $i = 1, 4$ (Fig. 3) directly with those known through the dynamic stiffness matrix D as described hereafter.³⁵

Dynamic Stiffness Matrix

First, the following displacement boundary conditions are prescribed:

$$\begin{aligned} W_1(-L/2) &= \delta_1, & W_2(-L/2) &= \delta_2 \\ W_1(L/2) &= \delta_3, & W_2(L/2) &= \delta_4 \end{aligned} \quad (12)$$

Substituting for W_1 and W_2 from Eqs. (10) and (11) gives

$$\begin{Bmatrix} \delta_1 \\ \delta_2 \\ \delta_3 \\ \delta_4 \end{Bmatrix} = \begin{bmatrix} C_1 & -S_1 & C_2 & -S_2 \\ f_1 C_1 & -f_1 S_1 & f_2 C_2 & -f_2 S_2 \\ C_1 & S_1 & C_2 & S_2 \\ f_1 C_1 & f_1 S_1 & f_2 C_2 & f_2 S_2 \end{bmatrix} \begin{Bmatrix} A_1^* \\ A_2^* \\ A_3^* \\ A_4^* \end{Bmatrix} \quad (13)$$

where

$$C_i = \cosh(\lambda_i L/2), \quad S_i = \sinh(\lambda_i L/2) \quad (14)$$

where $i = 1, 2$. Equation (13) can be inverted to yield the matrix equation in the form of

$$A^* = R\delta \quad (15)$$

The axial forces in the outer and inner tubes are found from Eqs. (3) and (4):

$$N_1(z) = J_1 W_1' + J_3 W_2', \quad N_2(z) = J_3 W_1' + J_2 W_2' \quad (16)$$

where

$$\begin{aligned} J_1 &= 2(A_1 r_1 h_1 + A_c a), & J_2 &= 2(A_2 r_2 h_2 + A_c b) \\ J_3 &= c A_c \end{aligned} \quad (17)$$

Next, the following force boundary conditions are prescribed:

$$\begin{aligned} N_1(-L/2) &= -F_1, & N_2(-L/2) &= -F_2 \\ N_1(L/2) &= F_3, & N_2(L/2) &= F_4 \end{aligned} \quad (18)$$

Substituting Eqs. (10) and (11) into Eqs. (16) and noting Eq. (18), we can write the resulting boundary conditions as

$$\begin{Bmatrix} F_1 \\ F_2 \\ F_3 \\ F_4 \end{Bmatrix} = \begin{bmatrix} d_1 S_1 & -d_1 C_1 & d_2 S_2 & -d_2 C_2 \\ d_3 S_1 & -d_3 C_1 & d_4 S_2 & -d_4 C_2 \\ d_1 S_1 & d_1 C_1 & d_2 S_2 & d_2 C_2 \\ d_3 S_1 & d_3 C_1 & d_4 S_2 & d_4 C_2 \end{bmatrix} \begin{Bmatrix} A_1^* \\ A_2^* \\ A_3^* \\ A_4^* \end{Bmatrix} \quad (19)$$

where

$$\begin{aligned} d_1 &= \lambda_1 (J_1 + J_3 f_1), & d_2 &= \lambda_2 (J_1 + J_3 f_2) \\ d_3 &= \lambda_1 (J_2 f_1 + J_3), & d_4 &= \lambda_2 (J_2 f_2 + J_3) \end{aligned} \quad (20)$$

C_i ($i = 1, 2$) and S_i ($i = 1, 2$) are given by Eq. (14). Equation (19) can be simply written as

$$F = SA^* \quad (21)$$

The dynamic stiffness matrix D is obtained by combining Eqs. (15) and (21) as

$$F = D\delta \quad (22)$$

$$D = SR \quad (23)$$

Equation (22) contains four degrees of freedom (DOF) corresponding to the two ends of the inner and outer tubes, as shown in Fig. 3. The damping mechanism section (composite section made of overlapping tube 1, damping material, and tube 2) is typically connected to adjacent elements at two DOF and is free at the remaining two DOF (Fig. 2). The axial forces corresponding to the two free DOF are zeros. For example, for the connection as shown in Fig. 2, F_2 and F_3 have zero values. The last step in the derivation now is to order the DOF, partition the 4×4 dynamic stiffness matrix, and condense out the DOF associated with the free ends. The ordering adopted in the present method puts the DOF at connected ends in rows 1 and 2 and the DOF at free ends in rows 3 and 4. For example, if the outer tube of the structural segment containing damping material is connected at the left to an adjacent element and is free on the right and the inner tube is connected at the right to another adjacent element and is free at the left (i.e., F_1 and F_4 are not zeros, whereas F_2 and F_3 are zeros), then Eq. (22) is ordered and partitioned as

$$\begin{Bmatrix} F_1 \\ F_4 \\ 0 \\ 0 \end{Bmatrix} = \begin{pmatrix} D_{11} & D_{12} \\ D_{21} & D_{22} \end{pmatrix} \begin{Bmatrix} \delta_1 \\ \delta_4 \\ \delta_2 \\ \delta_3 \end{Bmatrix} \quad (24)$$

This ordering is written as (1, 3, 4, 2) (see Figs. 2, 3, and 4c). Here, the location fields 1 and 4 (Fig. 4) have new values of 1 and 2, indicating that the DOF 1 and 4 are connected to adjacent elements, whereas location fields 2 and 3 are given new values of 3 and 4, indicating that DOF 2 and 3 are free. (Corresponding forces are zeros.) Here, D_{ij} are the partitioned 2×2 submatrices of the dynamic stiffness matrix.

Condensing out δ_2 and δ_3 yields the following 2×2 dynamic stiffness matrix for the section:

$$\begin{Bmatrix} F_1 \\ F_4 \end{Bmatrix} = [D_{11} - D_{12} D_{22}^{-1} D_{21}] \begin{Bmatrix} \delta_1 \\ \delta_4 \end{Bmatrix} \quad (25)$$

The ordering is specified for each section, which allows the sections to be connected in different configurations along the truss member length, as shown in Fig. 4. Moreover, if a section of the member does not contain the damping layer (left or right segment in Figs. 1a and 2), this configuration can also be represented by

the same formulation used for the section with the damping layer (middle segment in Figs. 1a and 2) by assigning zero values for density, modulus of elasticity, and Poisson’s ratio corresponding to the damping layer and the inner or outer tube, whichever is appropriate (Fig. 5). The dynamic stiffness matrices for each section are then assembled to find the equations for the super element representing an entire truss member with damping at a certain discrete location along the member length.

These features of the method presented provide tremendous versatility in modeling truss members with a variety of damping treatments along the length, such as discrete segmental damping treatment, continuous damping treatment, and damping layer as arranged in Figs. 6a–6d. The external arrangement of the damping layer (Figs. 6b and 6d) is the same as the widely known constrained layer damping.

Verification of Super Element

The solution for a concentric tubular section with a damping layer (damping element) presented earlier was verified by comparing the results with an analytical solution for a single-DOF (SDOF) os-

cillator and with a conventional finite element model.^{34,35} In these comparisons, the damping element was considered part of a three-element super element, as shown in Figs. 1a, 2, and 6c. The natural frequency and the effect of loss factor on displacements predicted by the present method agree closely with that of the SDOF oscillator. The verification with a conventional finite element model is performed using MARC Analysis Research Corporation software.³⁷ Two-dimensional, axisymmetric solid elements were used. Element aspect ratios were kept at 1:1 near the overlap region and increased to 5:1 in the interior section. Because of eccentricity of loading and interface shear, bending is introduced in the structure. Bending effects were neglected in the kinematic assumptions for the present solution. To study the effects of bending on the response, two different finite element analyses were performed. In the first, the model was supported radially only at the left and right ends, and in the second the entire model was radially constrained. The results show that, for the radially unconstrained model, the difference in natural frequencies is approximately 17%, and for the radially constrained model, the results agree within 1%. It is expected that the importance of bending will depend on the geometric and material parameters of the structure, which can be further investigated by additional parametric studies. Bending can be included in the kinematic assumptions, and the same solution procedure can be applied. However, the complexity of the equations will increase significantly.

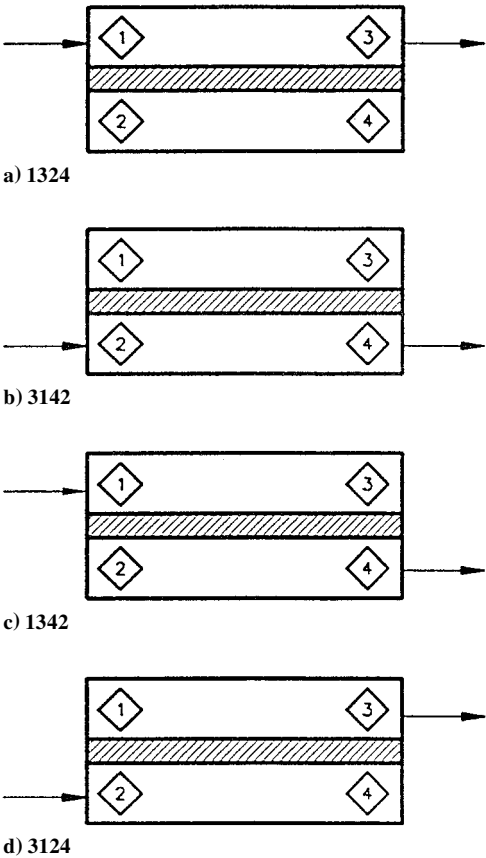


Fig. 4 Ordering of element DOF on a super element.

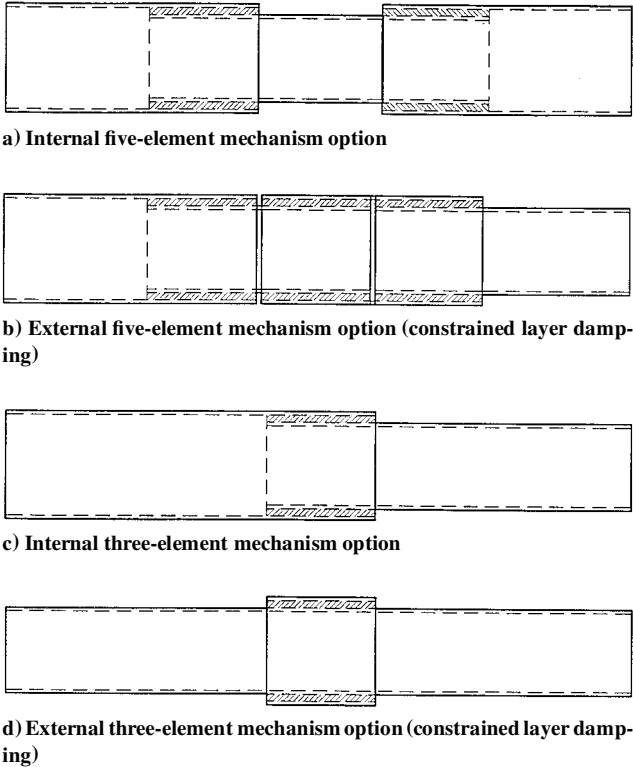


Fig. 6 Some possible damping schemes using the formulation.

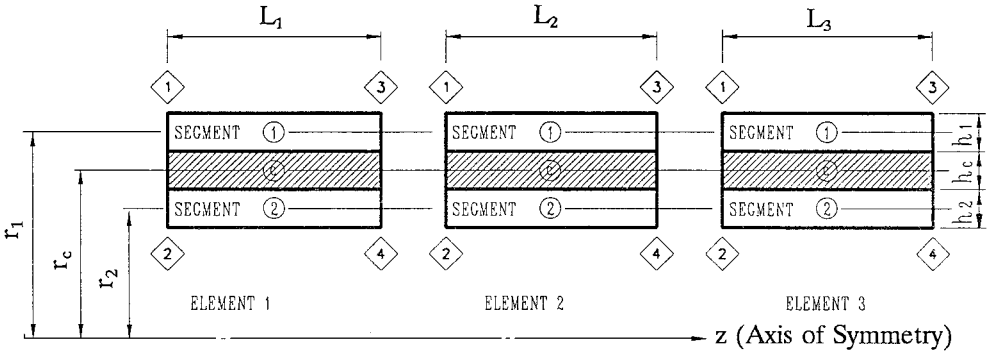


Fig. 5 Three-element, super-element representation.

Implementation of the Super Element in a Structure

The theory and the computer program for the damping mechanism were thus successfully verified and tested against the established MARC finite element code.³⁷ Now it is of interest to study the behavior of the super element in a structure. A program was written in FORTRAN to analyze the harmonic response of a two-dimensional, truss-type structure with members containing the damping elements.

The structure considered for the study was a 24-bay, truss-type structure, as shown in Fig. 7, with the following geometric dimensions: length $L = 77.590$ m, top chord bay spacing $S = 3.233$ m, and height $h = 4.572$ m. The length of the diagonal is equal to 4.849 m. The members located at the upper and lower chords are exact beam elements with axial and flexural properties. These members have a rectangular cross section with a 25.4-cm width and a 2.54-cm depth. All of the web members (verticals and diagonals) of the structure are truss members and are represented by super elements developed in this study. The super elements have three sections, the middle one being the damping element (Fig. 1a). The outer diameter of these members is equal to 30.734 cm. The thicknesses of the outer and inner tubes are constant at 0.254 cm. The thickness of the viscoelastic layer is either 0.254 or 0.0254 cm. The cross-sectional dimensions for sections 1–3 are as follows: thickness $h_1 = 0.254$ cm, $h_c = 0.254$ (or 0.0254) cm, and $h_2 = 0.254$ cm and radius $r_1 = 15.24$ cm, $r_c = 14.986$ (or 15.100) cm, and $r_2 = 14.732$ (or 14.9606) cm. All members of the structure are made of aluminum with the following properties (Table 1): modulus of elasticity $E = 69$ GPa, density $\rho = 2800$ kg/m³, and Poisson’s ratio $\nu = 0.30$. The storage modulus of elasticity of the viscous material $E_c^o = 2.07$ GPa. No damping mechanisms developed in this study are provided in the top and bottom chord members (longerons) because they are modeled as beam elements with flexural as well as axial stiffness. If these longerons were truss members, the viscous damping mechanism segments could have been used. Note, however, that the damping mechanism segments cause reduction in the stiffness of the members where they are used due to the presence of the viscous material in them.

Truss geometry, which includes the joint coordinates and connectivity, is generated within the program. Boundary conditions chosen for the truss place the truss on rollers at the two lower end joints and fixes the truss against horizontal translation at the center of the upper chord. The structure can be loaded with a harmonic vertical force at any joint in the assembly. For the present study, the structure is loaded by a harmonic load of magnitude of 1 kN in the vertical direction at the $\frac{1}{8}$ th length point from the left (node 4, Fig. 7). Because the program uses exact equations, there needs to be only one element per member to model properly the behavior of the entire structural member. The program developed here uses conventional subroutines for regular operations, such as assembly of elements, rotations, and matrix inversions.

Table 1 Material properties									
Section	Young’s modulus, GPa			Mass density, kg/m ³			Poisson’s ratio		
	E_1	E_c	E_2	ρ_1	ρ_c	ρ_2	ν_1	ν_c	ν_2
1	69	0	0	2800	0	0	0.3	0	0
2	69	2.07	69	2800	2800	2800	0.3	0.3	0.3
3	0	0	69	0	0	2800	0	0	0.3

Results and Discussion

This section first presents the verification of the method and the computer program developed in this study. This verification subsection is followed by results delineating effects of loss factor, thickness, and length of the viscoelastic layer on the behavior of the truss-type structure.

Frequency and Mode Shape Verification

The computer program developed in this study to analyze the truss-type structure was first tested against the MARC finite element code.³⁷ The first three frequencies and mode shapes of the two-dimensional truss structure shown in Fig. 7, with all members straight and without a damping mechanism, were obtained from both the computer program developed in this study and the MARC finite element code. The first, second, and third frequencies as obtained from the present program were approximately 2.0, 6.6, and 10.4 Hz, respectively, and those obtained from the MARC code were 2.16, 6.5, and 11.28 Hz (Table 2). Therefore, the differences in the first, second, and third frequencies obtained from these two methods are 8.0, 1.50, and 8.40%, respectively. The program developed in this study uses harmonic and frequency-domain analysis. A frequency sweep increment of 0.2 Hz was used in the computation of these frequencies. Given this somewhat coarser frequency sweep increment used in the program, the maximum difference in the frequency values of about 8% is very reasonable. Furthermore, the first and second mode shapes obtained from these two techniques are observed to match closely, as shown in Figs. 8 and 9. This verification, thus, establishes the level of accuracy of the computer program developed here.

Table 2 Comparison of natural frequencies of the structure

Mode	Current solution, Hz	MARC, Hz	Percent difference
1	2.0	2.16	8.0
2	6.6	6.50	1.5
3	10.4	11.28	8.4

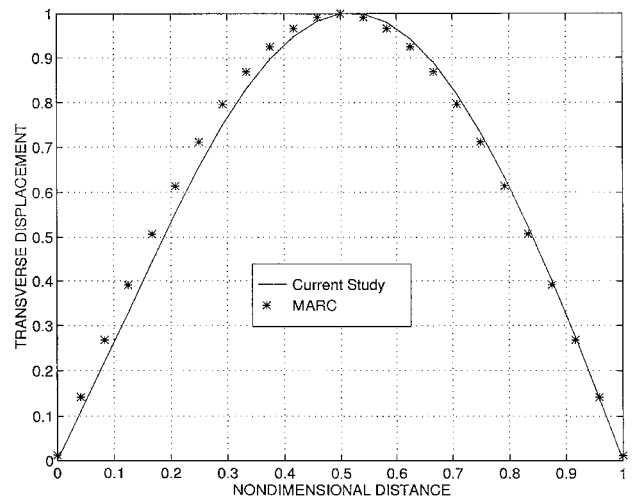


Fig. 8 First mode shape of the structure.

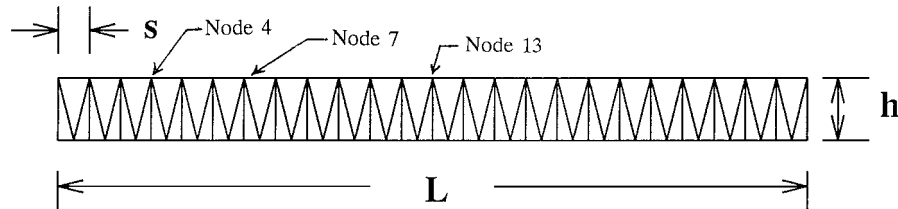


Fig. 7 Truss-type structure geometry.

Table 3 Parameters used in case studies

Case	Loss factor, η	Percent length of damping treatment	Thickness of damping layer h_c , cm
1	0.05	33	0.0254
2	0.01	33	0.0254
3	0.05	33	0.2540
4	0.05	50	0.0254
5	0.05	50	0.2540
6	0.10	33	0.0254
7	0.10	33	0.2540
8	0.10	50	0.0254
9	0.10	50	0.2540
10	0.70	33	0.0254
11	0.70	33	0.2540
12	0.70	50	0.0254
13	0.70	50	0.2540

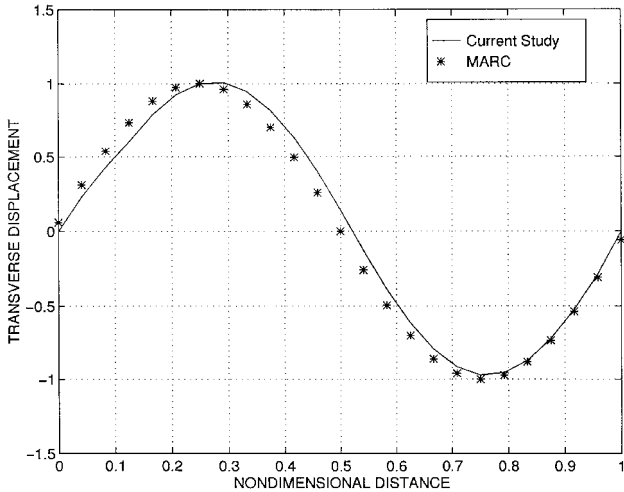


Fig. 9 Second mode shape of the structure.

Effects of Damping Element Parameters

After the successful testing, the program was utilized to study the effects of several values of loss factor, length, thickness, and percentage length of the viscoelastic layer on the behavior of the truss-type structure with the three-section super elements (Figs. 1 and 6c) used as the vertical and diagonal members. Table 3 gives the values of the parameters varied in the study. Vertical displacements of nodes 4, 7, and 13 of the structure (Fig. 7) are obtained as the structure is subjected to the frequency sweep at an interval of 0.01 Hz. The structure is loaded by a harmonic load of magnitude 1 kN in the vertical direction at the $\frac{1}{8}$ th length point from the left (node 4, Fig. 7). The results for node 13 are summarized in Fig. 10; these are representative of the first mode response. [Node 13, the midlength top chord point of the structure shown in Fig. 7, experiences maximum displacement for the first mode (see Fig. 9).] Figure 11 shows a representative plot of displacement vs frequency for case 1 (Table 3). Although the results presented in Fig. 11 are generated with a larger-frequency sweep of 0.1 Hz and do not represent the correct displacement values, Fig. 11 is provided to illustrate the overall trend of the displacements at three nodes (4, 7, and 13) as the frequency changes. Figure 12 shows the effects of the frequency sweep size (0.1 vs 0.01 Hz) on the displacement magnitude (case 1, node 13 for mode 1). The results presented in Fig. 10 are obtained for a finer-frequency sweep at an interval of 0.01 Hz and represent the more accurate magnitudes of displacements.

The very sharp response peak seen in Fig. 12 indicates a very lightly damped structure. This indicates that the placement of the damping struts on the verticals and diagonals is only lightly affecting the overall structural response.

The parametric study results (Fig. 10) show two levels of response. Cases with a shorter (33%), thin (0.0254-cm) damping layer, regardless of loss factor, show less damping effect and a larger re-

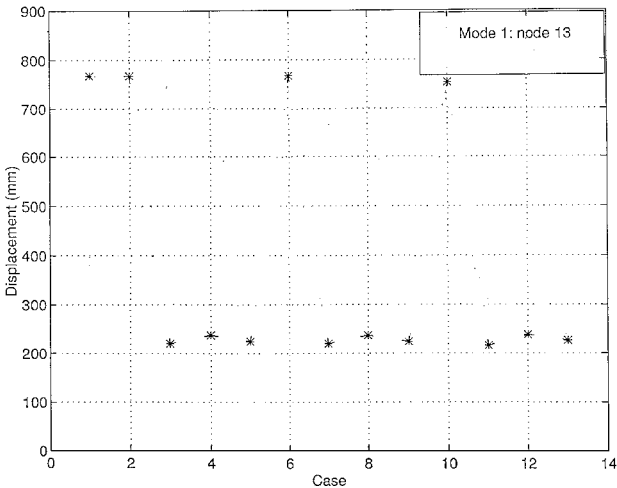


Fig. 10 Displacement vs case numbers.

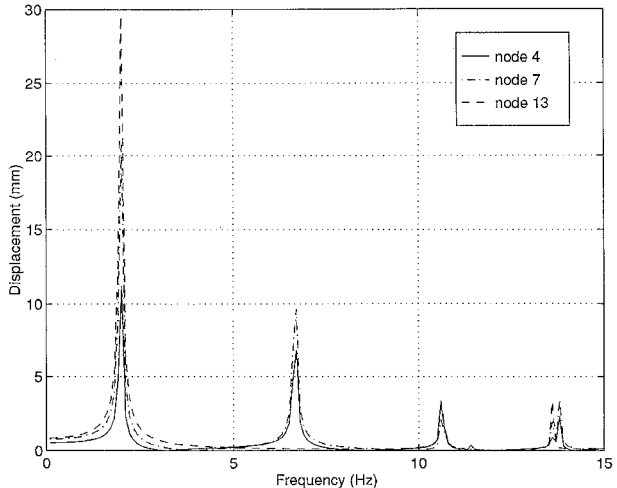


Fig. 11 Displacement vs frequency for case 1.

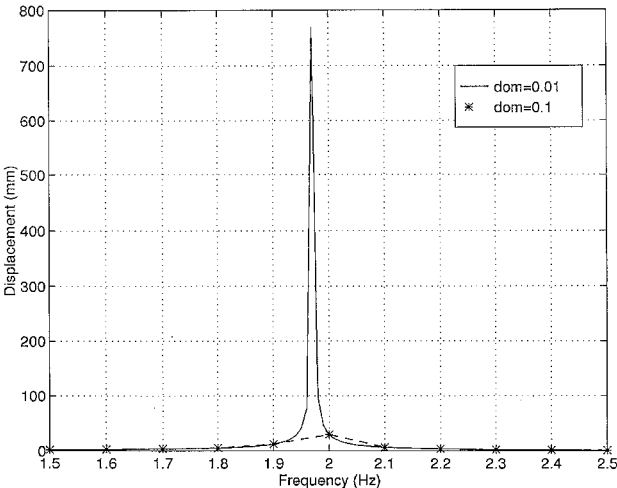


Fig. 12 Displacement vs frequency as a function of frequency sweep size (case 1, mode 1, node 13).

sponse. All other cases show more effective damping and a lesser response.

1) For the range of loss factors considered, the change in the loss factor of the viscoelastic element has only very small impact in the damping of the main structure.

2) For the first mode, an increase in the thickness of the damping layer from 0.0254 to 0.254 cm decreases the displacement of the structure when the damping layer length is 33%. However, no

significant change in the damping effect is noticed by increasing the damping layer thickness if the damping length is 50%.

3) As the length of damping material increases from 33 to 50%, the damping mechanism provides more effective damping on the structure (i.e., displacements decrease) for the first mode if the damping layer thickness is smaller (0.0254 cm). When the thickness is larger (0.254 cm), there is no significant change in the damping effect as the length is increased.

It must be pointed out that, because the structure selected has the damping mechanism employed in the diagonals and vertical members only, resulting in a lightly damped structure, there is a greater possibility of the results being influenced by numerical artifacts for lower modes. If the damping mechanism is provided on the chordal members of the truss-type structure instead of the diagonal and vertical members, the damping effects on the structure could be enhanced. However, this may have an added adverse effect of reduction in the stiffness of the structure.

Conclusions

A damping mechanism suitable for a tubular truss structural member of circular cross section is developed that incorporates the behavior of a viscoelastic layer. The mechanism calls for overlapping end portions of two tubes to be bonded together by means of a thin layer of viscoelastic material. A super element formulation is developed to represent a full length of a truss member consisting of one or more of such damping mechanism segments.

The element has been used to study the vibration suppression in a truss-type structure. The vibration suppression is studied for a range of frequencies. A parametric study has been performed to establish the effects of loss factors, thickness, and length of the damping material on a selected structure.

The damping characteristics of the mechanism developed can be complex and depend on a combination of loss factor, thickness, and length of the damping layer used. The damping effects on a structure using this mechanism may not, therefore, be observed to be as intuitive as expected for certain modes of vibration. The numerical scheme developed and presented here allows rapid parametric studies of these effects so that effective designs can be created.

Acknowledgment

This work was supported in part by the NASA/Connecticut Space Grant College Consortium through a graduate student fellowship to Hamid R. Adib-Jahromi.

References

- ¹Lazan, B. J., *Damping of Materials and Members in Structural Mechanics*, Pergamon, Elmsford, NY, 1968, pp. 35, 36.
- ²Beards, C. F., "Damping on Structural Joints," *Shock and Vibration Digest*, Vol. 11, No. 9, 1979, pp. 35–41.
- ³DiTanto, R. A., "Theory of the Vibratory Bending for Elastic and Viscoelastic Finite Length Beams," *Journal of Applied Mechanics*, Vol. 32, No. 4, 1965, pp. 881–886.
- ⁴Mead, D. J., and Markus, S., "The Forced Vibration of a Three-Layer Damped Sandwich Beam with Arbitrary Boundary Condition," *Journal of Sound and Vibration*, Vol. 10, No. 2, 1969, pp. 163–175.
- ⁵Renton, W., and Vinson, J., "Analysis of Adhesively Bonded Joints Between Panels of Composite Materials," *Journal of Applied Mechanics*, No. 1, 1977, pp. 101–106.
- ⁶Ojalvo, I. U., and Eidinoff, H., "Bond Thickness Effects upon Stresses in Single-Lap Adhesive Joints," *AIAA Journal*, Vol. 10, No. 3, 1978, pp. 204–211.
- ⁷Delale, F., and Erdogan, F., "Viscoelastic Analysis of Adhesively Bonded Joints," *Journal of Applied Mechanics*, Vol. 48, No. 2, 1981, pp. 331–336.
- ⁸Delale, F., Erdogan, F., and Aydioglu, M., "Stresses in Adhesively Bonded Joints—A Closed Form Solution," *Journal of Composite Materials*, Vol. 15, March–April 1981, pp. 101–106.
- ⁹Saito, H., and Tani, H., "Vibrations of Bonded Beams with Single-Lap Adhesive Joints," *Journal of Sound and Vibration*, Vol. 92, No. 2, 1984, pp. 299–309.
- ¹⁰Miles, R., and Reinhall, P., "An Analytical Model for the Vibration of Laminated Beams Including the Effects of Both Shear and Thickness Deformation in the Adhesive Layer," *Journal of Vibration, Acoustics, Stress, and Reliability in Design*, Vol. 108, No. 1, 1986, pp. 56–64.

- ¹¹Prucz, J., Reddy, A., Rehfield, L., and Trudell, R., "Experimental Characterization of Passively Damped Joints," *Journal of Spacecraft and Rockets*, Vol. 23, No. 6, 1986, pp. 568–575.
- ¹²Prucz, J., Kokkinos, F., and Spyarakos, C., "Advanced Joining Concepts for Passive Vibration Control," *Journal of Aerospace Engineering*, Vol. 1, No. 4, 1988, pp. 193–205.
- ¹³Rao, M. D., and Crocker, M., "Analytical and Experimental Study of the Vibration of Bonded Beams with a Lap Joint," *Journal of Vibration and Acoustics*, Vol. 12, No. 4, 1990, pp. 444–451.
- ¹⁴He, S., and Rao, M. D., "Longitudinal Vibration and Damping Analysis of Adhesively Bonded Double-Strap Joints," *Journal of Vibration and Acoustics*, Vol. 114, No. 3, 1992, pp. 330–337.
- ¹⁵He, S., and Rao, M. D., "Vibration Analysis of Adhesively Bonded Lap Joint, Part I—Theory," *Journal of Sound and Vibration*, Vol. 152, No. 3, 1992, pp. 405–416.
- ¹⁶He, S., and Rao, M. D., "Vibration Analysis of Adhesively Bonded Lap Joint, Part II—Numerical Solution," *Journal of Sound and Vibration*, Vol. 152, No. 3, 1992, pp. 417–425.
- ¹⁷Rao, M. D., and Zhou, H., "Vibration and Damping Analysis of a Scarf-Jointed Beam in Flexure," *Journal of the Acoustical Society of America*, Vol. 93, No. 4, Pt. 1, 1993, pp. 1918–1926.
- ¹⁸Crawley, E. F., "Nonlinear Characteristics of Joints as Elements of Multi-Body Dynamic Systems," *Computational Methods for Structural Mechanics and Dynamics*, NASA CP 3034, 1985.
- ¹⁹Belvin, W. K., "Modeling of Joints for the Dynamic Analysis of Truss Structures," NASA TP 2661, 1987.
- ²⁰Bowden, M., and Dugundji, J., "Effects of Joint Damping and Joint Nonlinearity on the Dynamics of Space Structures," AIAA Paper 88-2480, April 1988.
- ²¹Abrate, S., and Sun, C., "Continuum Modeling of Damping in Large Space Structures," *Proceedings of the 2nd International Conference on the Recent Advances in Structural Dynamics*, edited by M. Petyt and H. Wolfe, Vol. 2, Univ. of Southampton, Southampton, England, U.K., 1984, pp. 877–885.
- ²²McTavish, D., Hughes, P., Soucy, Y., and Graham, W., "Prediction and Measurement of Modal Damping Factors for Viscoelastic Space Structures," *AIAA Journal*, Vol. 30, No. 5, 1992, pp. 1392–1399.
- ²³McTavish, D. J., and Hughes, P. C., "Modeling of Linear Viscoelastic Space Structures," *Journal of Vibration and Acoustics*, Vol. 115, No. 1, 1993, pp. 103–110.
- ²⁴Sankar, B., and Deshpande, A. S., "Passive Damping of Large Space Structures," *AIAA Journal*, Vol. 31, No. 8, 1993, pp. 1511–1516.
- ²⁵Bush, H. G., Mikulas, M., and Heard, W., "Some Design Considerations for Large Space Structures," *AIAA Journal*, Vol. 16, No. 4, 1978, pp. 352–359.
- ²⁶Padula, S., Sandridge, C., Walsh, J., and Haftka, R., "Integrated Controls-Structures Optimization of a Large Space Structure," *Computers and Structures*, Vol. 42, No. 5, 1992, pp. 725–732.
- ²⁷Lubkins, J. L., and Reissner, E., "Stress Distribution and Design Data for Adhesive Lap Joints between Circular Tubes," *Transactions of the American Society of Mechanical Engineers*, Vol. 78, 1956, pp. 1213–1221.
- ²⁸Alwar, R. S., and Nagaraja, Y. R., "Viscoelastic Analysis of an Adhesive Tubular Joint," *Journal of Adhesion*, Vol. 8, No. 1, 1976, pp. 79–92.
- ²⁹Adams, R. D., and Peppiatt, N. A., "Stress Analysis of Bonded Tubular Lap Joints," *Journal of Adhesion*, Vol. 9, No. 1, 1977, pp. 1–18.
- ³⁰Chon, C. T., "Analysis of Tubular Lap Joint in Torsion," *Journal of Composite Materials*, Vol. 16, No. 4, 1982, pp. 268–283.
- ³¹Medri, G., "Viscoelastic Analysis of Adhesive Bonded Lap Joints Between Tubes Under Torsion," *Journal of Vibration, Acoustics, Stress, and Reliability in Design*, Vol. 110, No. 3, 1988, pp. 384–388.
- ³²Zhou, H., and Rao, M. D., "Viscoelastic Analysis of Bonded Tubular Joints Under Torsion," *International Journal of Solids and Structures*, Vol. 30, No. 16, 1993, pp. 2199–2211.
- ³³Rao, M. D., and Zhou, H., "Vibration and Damping of a Bonded Tubular Lap Joint," *Journal of Sound and Vibration*, Vol. 178, No. 5, 1994, pp. 577–590.
- ³⁴Adib-Jahromi, H., "Passive Damping of Truss Structures with Tubular Members," Ph.D. Dissertation, Dept. of Civil and Environmental Engineering, Univ. of Connecticut, Storrs, CT, March 1995.
- ³⁵Adib-Jahromi, H., Malla, R., and Accorsi, M., "Constrained Layer Damping of Tubular Truss Members," *AIAA Journal*, Vol. 34, No. 7, 1996, pp. 1487–1493.
- ³⁶Cremer, L., Heckl, M., and Ungar, E. E., "Damping," *Structure-Borne Sound*, 2nd ed., Springer-Verlag, New York, 1988, pp. 195–265.
- ³⁷MARC User's Manual, MARC Analysis Research Corp., Palo Alto, CA, 1993.

H. L. McManus
Associate Editor